Transport characteristics calculation of bilayer graphene with different misorientation angle

© S.V. Khazanova, V.V. Savel'ev

Lobachevsky State University,
603950 Nizhny Novgorod, Russia
E-mail: khazanova@phys.unn.ru

Received May 5, 2023
Revised June 29, 2023
Accepted July 6, 2023

In this work a bilayer moiré graphene structure with a spatial period of energy parameters change of the ten nanometers order is considered. The layer misorientation angle effect and the energy gap parameter on the current-voltage characteristic of the structure is studied numerically. The transmission coefficients calculation through the structure demonstrates the appearance of energy gaps, the magnitude of which depends on the misorientation angle of the layers.

Keywords: bilayer graphene, moiré pattern, Fermi velocity, transmission coefficient, negative differential conductivity.

DOI: 10.61011/SC.2023.05.57152.36k

1. Introduction

The main requirements for modern electronic devices are minimal size, high-speed response, and low power consumption, therefore the components of such devices should be based on materials with reduced dimensionality and high mobility of charge carriers. The creation of two-dimensional materials has recently attracted great interest [1]. In particular, of interest is graphene, a monolayer of carbon atoms with a number of unique properties, such as excellent electrical conductivity at room temperature, high mobility, thermal conductivity, strength, and transparency. At the same time, one of the disadvantages of an isolated graphene monolayer is the lack of the band gap required to control the electronic transport of devices. It is known that applying an electric field perpendicular to the sheet plane [2], creating a periodic potential in graphene by doping it or applying it onto a substrate with periodic properties in the lateral plane [3] results in the emergence of an energy slot, which makes it possible to implement high-speed semiconductor devices of a new generation based on it.

Also, the disadvantages of single graphene sheet can be removed by using structures of two or more layers of two-dimensional materials with different parameters. When using multilayer graphene, the advantages of monolayer graphene are retained; in particular, when applied to a substrate, it provides conductivity through the lower layer [4]. At the same time, the bilayer graphene has features that distinguish it from the monolayer, such as the presence of a band gap. The ability to address each layer separately leads to entirely new functionalities of the bilayer graphene, including control of the band gap of up to ~ 300 meV by doping or applying external voltage.

Additional possibilities open up when using a number graphene sheets offset relative to each other in the plane. When two layers of graphene are offset with their corresponding crystallographic axes in the lateral plane arranged at a certain angle (the misorientation angle), a moiré-like pattern arises, periodically arranged regions with different crystallographic structures appear (so-called AA packing and AB packing, also known as Bernal packing) (Figure 1, *a*), and the properties of graphene change periodically. Regions with AA packing exhibit semimetallic properties, while AB packings demostrate semiconductor properties with a band gap of ~ 10 meV. In addition, when sheets are superimposed, their interaction causes relaxation of the lattice, which results in a decrease in the size of AA regions and, as a consequence, in an increase in AB regions [5,6]. The presence of a geometric superperiod in a graphene bilayer also leads to changes in the energy structure, and the parameters of the superperiod depend on the misorientation angle. Also, various theoretical groups have shown that for the smallest rotation angles θ, flat zones appear in the spectrum, which leads to electronic localization (a very low Fermi velocity). In other words, bilayer graphene is a very complex structure that can behave differently (ballistic motion or electron confinement) depending on the angle of rotation. Taking into account that the graphene phase with the AA type packing is metastable, alternating different packings makes the structure more stable and provides greater opportunities for creating devices based on them. In particular, these structures can be used for highly sensitive optoelectronics due to the appearance of Van Hove singularities in the electron density of states [7]. Devices developed on the basis of such graphene objects open a new field of electronics known as „twistronics“ [8,9].

2. Object under study

The structure under study is a moiré graphene with small misorientation angles ($\Theta = 0.88$ and 1.2°) ($\Theta = 0.88^\circ$ in Figure 1, *b* left). Our model of bilayer moiré graphene assumes that the energy properties of one graphene layer are modulated by the second layer rotated in the plane relative to the first layer by a given angle. Let us assume that in regions with AA packing the Δ bandgap parameter is equal to 0, and in AB regions it is non-zero. Thus, the bottom of the conduction band in the plane of moiré graphene is periodically modulated with a period of ~ 10 nm (see Figure 1, *b*). Then an assumption can be made that in type AA regions localization of electron wave functions takes place [10], which suggests the possibility of considering transport via quantum states.

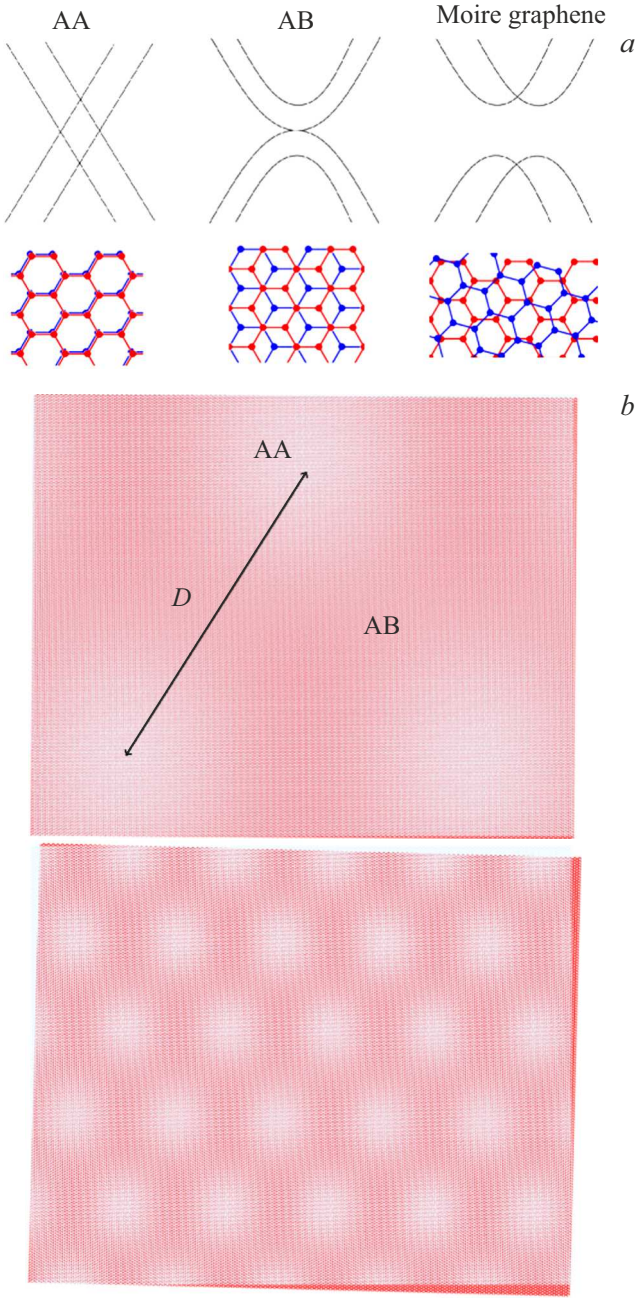

Figure 1. *a* — structure and energy band diagrams of AA and AB packings of graphene, energy band diagram of moiré graphene at the*K* point; *b* — image of moiré graphene at misorientation angles of 0.88° (left) and 3° (right). (The colored version of the figure is available on-line).

It is known that the dispersion dependence of a free graphene sheet is linear. Figure 1, *a* shows the structure and energy band diagrams of ideal AA and AB packings of graphene. The development of structures based on bilayer graphene with a certain geometry leads to the appearance of an energy gap similar to the band gap [11,12]. Figure 1, *b* shows models of moiré graphene sheets of the same size for misorientation angles of $\Theta = 0.88$ and 3°. Patterns formed when two sheets are offset, or the so-called „moiré“ patterns, have a period D, depending on this angle

$$D = \frac{a}{2\sin\left(\frac{\theta}{2}\right)},$$

where a is graphene lattice constant, $a \sim 0.246$ nm [13].

Light areas in Figure 1, *b* correspond to the structure with AA packing, dark areas correspond to AB. Moreover, due to the decrease in symmetry and removal of degeneracy, the energy band structure of moiré graphene has a more complex form. Its distinctive feature is the possibility of the existence of a band gap at the point K for an ideal structure [8] (Figure 1, *a*). Due to the fact that biaxial stretching of graphene does not result in the formation of a band gap in it [14], even despite the presence of mechanical stresses, the AA regions can retain semimetallic properties. Thus, one of the options for creating a period in the energy structure is to alternate graphene regions with a band gap and regions without a band gap (see the inset in Figure 2). The energy gap arising in these regions with semiconductor properties is described by the Δ parameter ($E_g = 2\Delta$) [15]. To mathematically describe the moiré graphene, a model of a periodic structure with 6 periods is used. The barrier width is determined by the moiré period and is $D/2 = 8$ nm, the bandgap parameter is $\Delta = 0.04$ eV, the Fermi level is $E_F = \Delta/2$.

3. Mathematical model

The effect of parameters of the moiré graphene on the current-voltage curve was studied by calculating the transmission coefficients for a given range of voltages applied to the structure. The transmission coefficient is calculated numerically using the transfer matrix method, taking into account features of the graphene structure [16]. It is known that energy states in graphene are described using the Dirac equation:

$$\hat{H} = v_F \boldsymbol{\sigma} \mathbf{p} + V(x)\hat{I}.$$

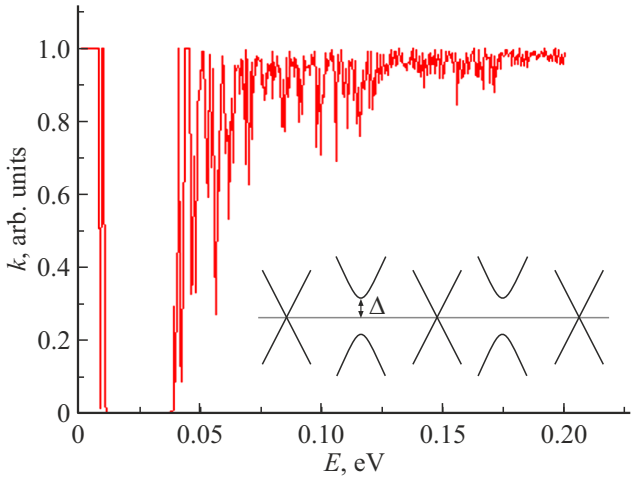

Figure 2. Spectrum of the transmission coefficient for the moiré graphene without taking into account relaxation for different bandgap parameters. The inset shows a model of the energy band diagram in the direction of the structure plane.

The solution to the Dirac equation can be represented in the form of spinors, the components of which describe the wave functions in two sublattices:

$$\psi_1(x) = \begin{pmatrix} 1 \\ se^{i\phi} \end{pmatrix} e^{ikx}; \quad \psi_2(x) = \begin{pmatrix} 1 \\ -se^{i\phi} \end{pmatrix} e^{-ikx}.$$

Let us introduce matrices that describe the behavior of the wave function inside the barrier and at its boundaries:

$$G = \begin{pmatrix} 1 & 1 \\ se^{i\phi} & -se^{-i\phi} \end{pmatrix}, \quad T(x) = \begin{pmatrix} e^{i\lambda x} & 1 \\ 1 & e^{-i\lambda x} \end{pmatrix}.$$

By expressing the matrix of transmission through a unit barrier: $S = G_b T_b^{-1} G_b^{-1}$, we obtain the matrix of transmission through the entire structure: $M = G^{-1}(\prod_n S_n)G$. In an arbitrary case, a wave falls on a graphene plane with alternating properties at a certain angle. For these calculations, the angle of incidence was taken to be $\varphi = 30^\circ$ [16].

The probability of penetration through a multi-barrier structure is determined by the diagonal element of the transfer matrix: $T(E) = |M_{22}|^{-2}$.

Thus, by calculating the transmission coefficients for each voltage and integrating, it is possible to calculate the current-voltage curve of the structure within the Landauer formalism [17]:

$$I = \frac{e}{4\pi^3\hbar} \int T(E)\big(f(E) - f(E')\big)dE,$$

where $E' = E + eU$ is energy of the unoccupied state, U is voltage applied to the structure, $f(E)$ is Fermi $-$Dirac distribution function [18].

Calculations of energy band diagrams [19,20] show that in moiré graphene the Fermi velocity near the Dirac point is renormalized and the degree of decrease in the velocity depends on the misorientation angle. For example, for the angle of $\Theta = 0.88^\circ$ the Fermi velocity is equal to 0.02 of the Fermi velocity of a free graphene sheet, and for the angle of $\Theta = 1.2^\circ - 0.03$ it is equal to 0.02 of the Fermi velocity ($2 \cdot 10^4$ m/s and $3 \cdot 10^4$ m/s, respectively). Low values of the Fermi velocity are associated with the emergence of a flat band mode, when states are strongly localized, predominantly in the AA moiré zones. In addition, due to structural relaxation, the potential wells where localization occurs become narrower, and the barriers widen and become sharper. Therefore, to describe the shape of the potential in structures with relaxation, a periodic function with constant energies in the regions corresponding to the AA and AB packings was used. The Δ parameter along the structure was modulated by this function.

4. Calculation results and discussion

For the selected model, transmission coefficients were calculated for various moire periods and energy parameters. Figure 2 shows the dependences of the transmission coefficient on energy for the model of moiré graphene without taking into account relaxation (applied voltage $U = 0.07$ V, $\Delta = 0.05$ eV). It can be seen in Figure 2, that in the transmission spectrum a region with low values of the transmission coefficient arises, which is interpreted as a forbidden region.

Then, the model took into account possible relaxation processes occurring in the structure of moiré graphene. Current-voltage curves (IU-curves) were obtained for periods of $D = 16$ and 11.76 nm (for $\Theta = 0.88$ and 1.2°, respectively), the current was calculated in $1.23 \cdot 10^{-5}$ A units (Figure 3). Figure 4 shows current-voltage curves calculated for various parameters of the band gap. It can be seen from the results, that the section of reverse differential resistance depends on both the misorientation angle and the

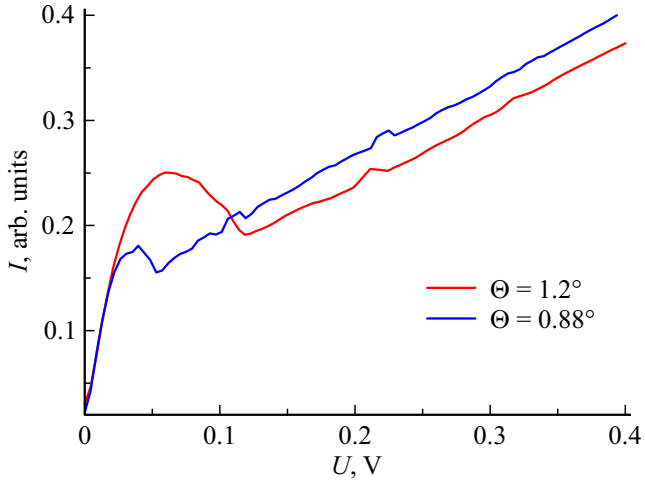

Figure 3. Current-voltage curves for structures with different misorientation angles of layers.

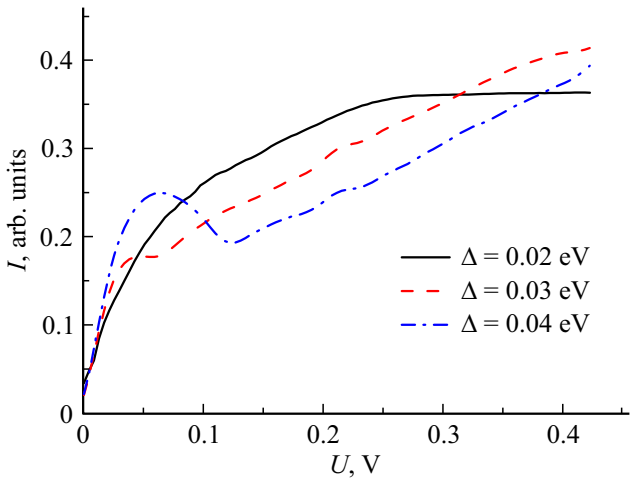

Figure 4. Current-voltage curves for structures with different band gap parameters in the regions with AB packing.

energy parameter. With increase in the band gap parameter, this region appears later in voltage and becomes more pronounced. It should be noted that the literature mentions devices created on the basis of moiré graphene [9] with the CU-curves having sections of reverse differential resistance.

5. Conclusion

In the structures of bilayer graphene, due to the offset of the layers relative to each other, a periodic potential of nanometer size arises, resulting in alternation of regions with different crystal packing and modulated band gap. Calculation of the transmission coefficients through this structure demonstrates the appearance of band gaps with magnitude depending on the angle of the layers offset. Current-voltage curves built on the basis of transmission coefficients for a smoothly varying applied voltage have sections with negative differential resistance, the position of which largely depends on the parameters of the structure.

Conflict of interest

The authors declare that they have no conflict of interest.

References

[1] A.C. Ferrari, F. Bonaccorso, V. Fal'ko, K.S. Novoselov. Nanoscale, **7**, 4598 (2015).
[2] A. Díaz-Fernández, L. Chico, J.W. González, F. Domínguez-Adame. ScentIfic Reports, **7**, 8058 (2017).
[3] C. Hwang, D.A. Siegel, S.-K. Mo, W. Regan. ScentIfic Reports, **2** (590), 1 (2012).
[4] J. Hass, F. Varchon, J.E. Millan-Otoya, M. Sprinkle, N. Sharma, W.A. de Heer, C. Berger, P.N. First, L. Magaud, E.H. Conrad. Rev. Lett., **100**, 125504 (2008).
[5] Nguyen N.T. Nam, Mikito Koshino. Phys. Rev. B, **96**, 075311 (2017).
[6] D.A. Bahamon, G. Gómez-Santos, T. Stauber. Nanoscale, **12**, 15383 (2020).
[7] T.B. Limbu, K. R. Hahn, F. Mendoza, S. Sahoo. Carbon, **117**, 367 (2017).
[8] A.V. Rozhkov, A.O. Sboychakov, A.L. Rakhmanov, F. Nori. Phys. Rep., **648**, 1 (2016).
[9] D.A. Ghazaryan, A. Misra, E.E. Vdovin, K. Watanabe. Appl. Phys. Lett., **118**, 183106 (2021).
[10] G.T. de Laissardiére, D. Mayou, L. Magaud. Phys. Rev. B, **86**, 125413 (2012).
[11] E. McCann, M. Koshino. Rep. Progr. Phys., **76**, 056503 (2003).
[12] Kin Fai Mak, Matthew Y. Sfeir, James A. Misewich, Tony F. Heinz. PNAS, **34**, 14999 (2010).
[13] J. Wang, W. Bo, Y. Ding, X. Wang. Mater. Today Phys., **14**, 100238 (2020).
[14] K.P. Katin, K.S. Krylov, M.M. Maslov, V.D. Mur. Diamond Relat. Mater., **100**, 107566 (2019).
[15] J.V. Gomes, N.M.R. Peres. J. Phys.: Condens. Matter, **20**, 325221-1 (2008).
[16] K. Uchida, S. Furuya, J.-I. Iwata, A. Oshiyama. Phys. Rew. B, **90**, 155451 (2014).
[17] Yu.M. Kardona. *Osnovy fiziki poluprovodnikov* (M., Fizmatlit, 2002). (in Russian).
[18] S. Dubey, V. Singh, Ajay K. Bhat, P. Parikh. Nano Lett., **13**, 3990 (2013).
[19] G. Alymov, V. Vyurkov, V. Ryzhii, D. Svintsov. Sci. Rep., **6**, 24654 (2016).
[20] E. Suárez Morell, J.D. Correa, P. Vargas, M. Pacheco, Z. Barticevic. Phys. Rew. B, **82**, 121407 (2010).

Translated by Y.Alekseev